Rail Wear Estimation for Predictive Maintenance: a strategic approach

Annemieke Meghoe, Richard Loendersloot, Rob Bosman and Tiedo Tinga

University of Twente, Enschede, 7522 NB, Netherlands
a.a.meghoe@utwente.nl
r.loendersloot@utwente.nl
r.bosman@utwente.nl
t.tinga@utwente.nl

ABSTRACT

Since the very beginning of rail transport, wear has been identified as one of the dominant damage mechanisms that influence the Remaining Useful Life (RUL) of rail tracks. Whereas maintenance of the track is now predominantly executed at fixed intervals or based on yearly inspections, the accurate prediction of rail wear could considerably improve the maintenance process. The present work proposes a method for long-term rail wear prediction using measurements of actual rail and wheel profiles as starting point. By doing so, the computational expensive step of updating the rail profile in a wear calculation, as is done in presently used methods, can be omitted. The proposed method is used to study a number of generic trends, varying curve radius and rail or wheel profile. Further, the method is validated against measured wear on actual track sections for moderate curves. Finally, it can easily be extended to include variations in operational usage of the track (type / weight of trains, geometric details, slip conditions) in the future. The method presented in this paper can therefore assist in improving the track maintenance process by maximizing the utilization of the track service life, and minimizing maintenance costs.

1. INTRODUCTION

Railway tracks have always been affected by wear and until now asset owners and track-maintainers continue to struggle to effectively address this. As wear cannot be prevented, the ability to predict the amount of wear could lead to maintenance planning optimization and cost reduction. Rail and wheel wear prediction started four decades ago with the first models primarily based on laboratory and field tests. With ever increasing computation power, numerical wear prediction models became more relevant. Wheel/rail wear prediction tools are incomplete without multi-body dynamics and rolling contact models. The multi-body simulation model is used to analyze the dynamic behavior during vehicle-track interaction and yields the contact forces and contact points. The obtained information serves as input to the local wheel-rail contact model to determine contact conditions, such as the amount of slip and the contact pressure distribution in the contact area. Finally, wear models are used to assess the degradation rates of the track.

Most of the wear prediction tools were developed for wheels rather than for rails (Pearce & Sherratt, 1991; Jendel, 2002; Ward, Lewis, & Dwyer-Joyce, 2003). Zobory (1997) was one of the few in that time to consider both wheel and rail profile wear. In 2005, Enblom developed a wear prediction tool for wheel profile evolution and even proposed one for rail profile evolution. The same methodology used for the wheel profile evolution was applied for the rail profile evolution under the assumption that the wear is uniform and the profile evolution is constant over the track. However, comparison of the simulation results with actual measurements showed that the wear rate was overestimated (Enblom & Berg, 2008). The results from the trial simulation did not correspond to the measured wear depths but the shape of the profiles were similar to those measured. The authors argued that the difference is due to the wear coefficient and environmental influences such as lubrication. They also argued that the difference could be due to the Hertzian contact theory used in the simulation, which lead to an overestimation of the contact pressures. Orvnas (2005) also simulated the rail profile evolution for the Swedish light rail line, but the results were merely qualitatively correct. The total wear was compared to the traffic tonnage and the results did not agree well with the field measurements. The recommendation given by Orvnas and later by Enblom and Berg (2008) is to increase the scaling of the wear coefficients. The wear coefficients used by Orvnas were scaled down by a factor of 5.6 and 11 for natural and artificial lubrication. respec-

Annemieke Meghoe et al. This is an open-access article distributed under the terms of the Creative Commons Attribution 3.0 United States License, which permits unrestricted use, distribution, and reproduction in any medium, provided the original author and source are credited.

tively.

From the literature, it can be concluded that rail wear prediction remains a challenging subject and application in rail maintenance optimization has not yet been achieved. Apart from the mismatch between amount of simulated and measured rail wear, previous researchers only considered sharp curved tracks (curve radii smaller than 800 meters). This research is sponsored by Strukton Rail who maintains a large part of the Dutch rail infrastructure that mostly consists of moderate curves. For this reason the focus of this paper will be only on tracks with curve radii between 1000 and 4000 meters. Furthermore, the use of new wheel and new rail profiles are suggested as initial conditions in previous approaches. These initial profiles are modified and updated after a certain amount of wear is predicted. The disadvantage of these approaches is the required computation time for the profile update. The method proposed in this paper avoids the profile update procedure and simulates wheel profiles in both new and worn conditions using measured rail profiles. Furthermore, a validation of the proposed method with measurements on a real track section is presented, demonstrating the potential of the proposed method in maintenance optimization.

2. METHODOLOGY

Figure 1 shows the four steps for typical wheel/rail wear analyses with the required input from track and vehicle data. In case of using the profile update procedure a new rail profile is inserted as the initial rail profile and the rail profiles are considered to be uniform along the track. The methodology proposed in this study discards the rail profile update step and substitutes the initial rail profiles with measured profiles, which can also vary along the track. This section describes the process and models from multi-body dynamic simulation to wear depth calculation and gives an overview of the approach followed for the simulations. Furthermore, an overview of rail profile measurement and analysis is presented.

2.1. Multi-Body Dynamics Model

Multi-body simulations are performed in order to predict the dynamic variation of contact forces and contact points during wheel-rail interaction. These simulations can be conducted with various commercially available multi-body software packages. During this study the commercially available software package VI-Rail is used. This software contains built in vehicle templates that can be adjusted accordingly (*VI-Rail 17.0 Documentation*, 2016). The vehicles then consist of car bodies, bogies and wheelsets which are considered as rigid bodies and are connected to each other by means of primary and secondary suspensions. The track model can easily be built up by choosing the track geometry parameters like length, rail inclination, rail cant etc. (see Figures 8 and 9), and the wheel and rail profiles are inserted as discrete

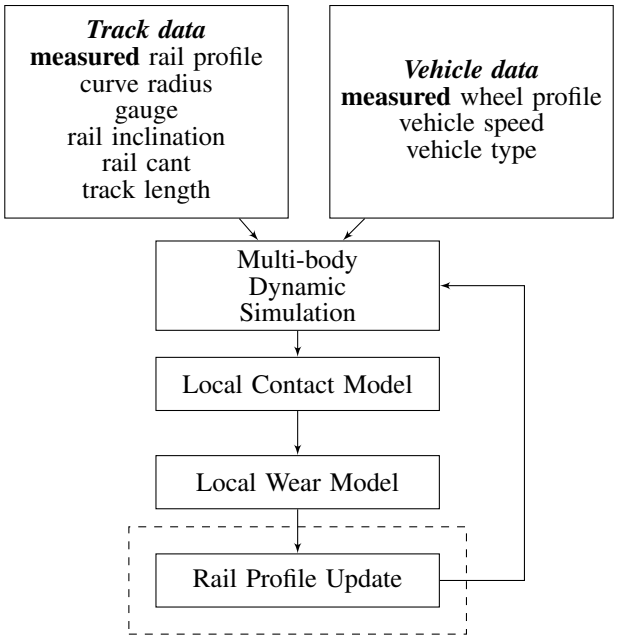

Figure 1. Process of rail wear prediction.

points. Furthermore, a general contact element method between wheel and rail is used that uses the exact wheel-rail geometry and permits multiple contact points. At each computation step the following contact parameters (as will be explained in more detail in 2.2) are extracted, for each contact point:

- Longitudinal and lateral creepage, and spin (γ_x, γ_y and ϕ)
- Maximum normal contact load (F_N) between wheel and rail
- Semi-axes a and b of the elliptical contact

The contact parameters for the complete time period resulting from the multi-body dynamic simulation are extracted and exported to a self-implemented Matlab script for the local contact and wear analysis.

2.2. Contact Model

The local contact model is based on the simplified rolling contact theory developed by Kalker (1990) where the wheel-rail contact can be described as pure rolling or pure sliding, or a combination of the two. For rolling and sliding motion, the contact area is divided into an adhesion (stick) zone and a slip zone. These zones originate from material points deformation within the contact area. Some points at the interface of the wheel stick to points of the track, and this part of the contact area is termed the stick zone. However, in other regions of the contact area, wheel material points move relative to the track points, thus forming a slip zone. The relative velocity between wheel material and track points is known as slip or slip velocity. The slip velocity divided by the vehicle

speed is regarded as creepage. Spin is defined as the relative angular velocity of the wheel normal to the contact plane divided by the vehicle speed (Sichani, 2016) and thus expresses the relative rotation of the contact area (Iwnicki, 2006).

The elliptical contact area defined by semi-axes a and b, is discretized into $N \times N$ elements; This enables to determine for each element whether it belongs to the stick or slip zone by comparing the tangential stress q_t for each element with the traction bound g. Figure 2 shows this procedure step by step.

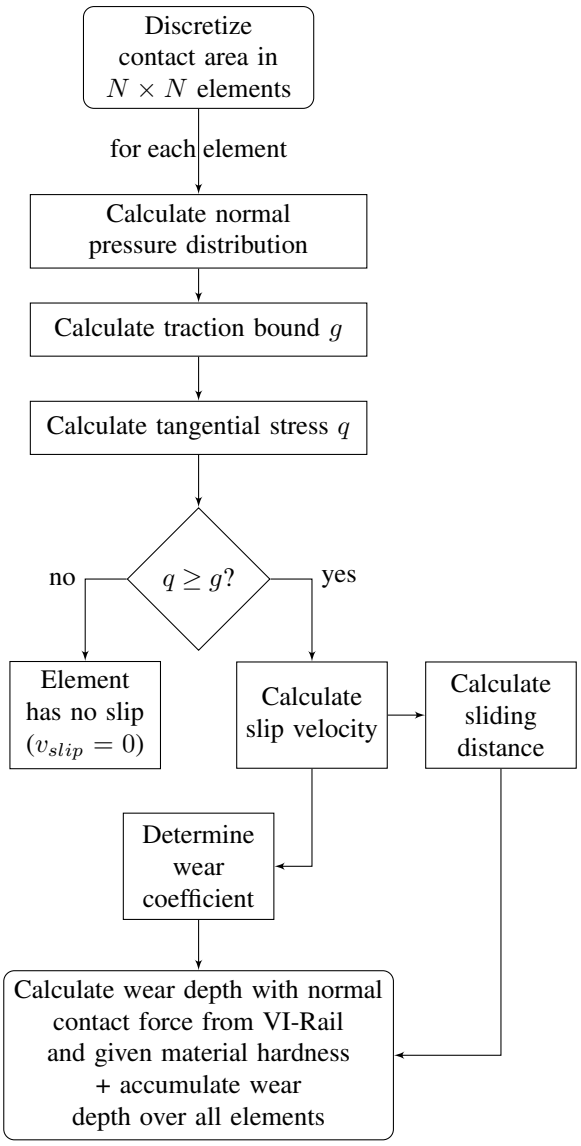

Figure 2. Wear depth calculation step by step for a contact area.

If the tangential stress is lower or equal to the traction bound, the element is in the stick zone but if it exceeds the traction bound the element is in the slip zone (Sichani, 2016). The traction bound is given by:

$$g(x, y) = \mu p(x, y) \tag{1}$$

where μ is the coefficient of friction and p the normal contact pressure distribution. The contact area is assumed to be of elliptical form with a semi-axis a in the longitudinal direction (the rolling direction of the vehicle) and the semi-axis b in the lateral direction. The maximum Hertzian contact pressure is calculated by:

$$p_{max} = \frac{3F_N}{2\pi ab} \tag{2}$$

The normal and tangential stress distributions are then given by:

$$p(x, y) = p_{max}\sqrt{1 - \frac{x^2}{a^2} - \frac{y^2}{b^2}} \tag{3}$$

$$q_t(x, y) = \sqrt{q_x(x, y)^2 + q_y(x, y)^2} \tag{4}$$

where the tangential stresses depend on the creepage and slip:

$$q_x(x, y) = \left[\gamma_x(x - a(y)) - \phi(x - a(y))y\right]/L \tag{5}$$

$$q_y(x, y) = \left[\gamma_y(x - a(y)) + \phi(x^2 - a^2(y))/2\right]/L \tag{6}$$

where $a(y)$ is half the length of the contact ellipse in longitudinal direction at location y and L is a single weighted parameter introduced by Kalker (1990):

$$L = \frac{L_x |\gamma_x| + L_y |\gamma_y| + L_\phi |\phi| c}{\sqrt{{\gamma_x}^2 + {\gamma_y}^2 + (\phi c)^2}} \tag{7}$$

where L_x, L_y and L_ϕ are material dependent equivalent lengths as defined below and $c = \sqrt{ab}$.

$$L_x = \frac{8a}{3GC_{11}} \tag{8}$$

$$L_y = \frac{8a}{3GC_{22}} \tag{9}$$

$$L_\phi = \frac{\pi a^2}{4GcC_{23}} \tag{10}$$

where G is the shear modulus, C_{11}, C_{22} and C_{23} are known as Kalker's creepage coefficients and are tabulated in the appendix published by Kalker (1990) for various ratios between semi-axes a and b and various Possion ratio.

2.3. Wear Model

Wear is related to material volume loss and can be divided in several types of wear mechanisms such as abrasive, adhesive, corrosive and surface fatigue wear (Li & Kalker, 1998). In the case of wheel-rail interaction, adhesive wear is the most commonly observed wear mechanism (De Arizon, Verlinden, & Dehombreux, 2007). Therefore the local wear model used in this research is based on the Archard's law for adhesive

wear (Archard, 1953). Archard demonstrated that the amount of wear volume loss V is proportional to the sliding distance s and normal contact load F_N through a wear coefficient K and that is inversely proportional to the hardness of the material H:

$$V = K\frac{sF_N}{H} \tag{11}$$

The wear coefficient K depends on the surface conditions and is usually determined empirically e.g. with pin-on-disk configuration measurements (Jendel, 2002; Lewis & Olofsson, 2004). For wear calculations regarding the current study the wear coefficient is estimated from the wear map published by Jendel (2002), see Figure 3. This map was constructed from a series of laboratory experiments for various contact pressures, sliding velocities and hardnesses of the material under dry conditions. Hence, the wear coefficient is a function of the contact pressure and the sliding velocity. The contact pressure can be extracted from the results yielded by the contact model and the sliding velocity can be calculated as (Enblom, 2005; Sichani, 2016):

$$|v| = \sqrt{(v_x)^2 + (v_y)^2} \tag{12}$$

where,

$$v_x(x,y) = V_{vehicle}(\gamma_x - \phi y) \tag{13}$$

$$v_y(x,y) = V_{vehicle}(\gamma_y + \phi x) \tag{14}$$

and $V_{vehicle}$ is equal to the vehicle speed.

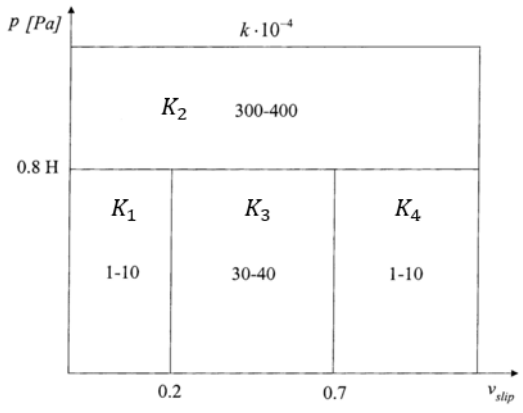

Figure 3. Jendel's wear map (Jendel, 2002).

The wear depth h for every discretized element in the elliptical contact is calculated by dividing Eq. 11 by the contact area which is assumed to be constant:

$$h = K\frac{sp}{H} \tag{15}$$

If the specific element is in slip, the sliding distance can be calculated as:

$$s = \frac{dx}{V_{vehicle}}|v| \tag{16}$$

where dx is the longitudinal element length, which is passed by the moving wheel in a time period $t = \frac{dx}{V_{vehicle}}$.

The wear depth is accumulated along the longitudinal direction, which results into the wear depth as function of the lateral coordinates of the contact ellipse. The worn area per contact ellipse is then determined as the integral of the accumulated wear depth over the lateral direction (i.e. wear depth multiplied by the length of contact ellipse in lateral direction, which is equal to 2 times semi-axes b).

2.4. Approach

Two sets of simulations were performed during this study. The first set of simulations were intended to gain insight and gather knowledge about the influence of the vehicle's dynamic behavior on the wear rate. Furthermore, this model also functions as the reference case which includes the basic requirements to perform a successful simulation. Hence, the model developed for this purpose is hereafter referred as the 'Basic Model'. The second set of simulations is performed to validate the accuracy of the proposed method by means of a case study. Figure 4 depicts the built-in vehicle template in VI-Rail, the ERRI Wagon, which has been used in the simulations of both the basic model and the case study. The vehicle characteristics are given in the appendix.

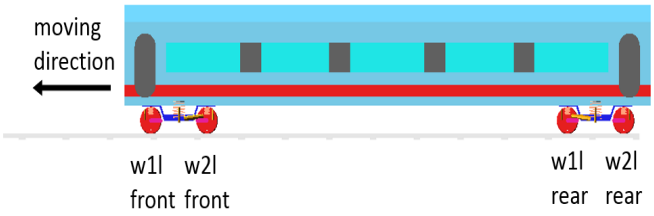

Figure 4. Schematic representation of the ERRI Wagon from the left side (see Appendix for details).

2.4.1. Basic model

The contact interface between wheel and rail has a major influence on the dynamic behavior. This contact interface is defined by the wheel and rail profile geometry. Changes in dynamic behavior yield varying contact forces and contact points, hence increasing wear rates. The problem of wheel-rail interface optimization has been addressed by several researchers and they also proposed methods to minimize the effect of the dynamic behavior by optimizing the wheel profile (Shevtsov, 2008; Santamaria, Herreros, Vadillo, & Correa, 2013; Ignesti, Innocenti, Marini, Meli, & Rindi, 2014). However, the wheel profile optimizations are mostly applicable to the specific cases and conditions that were studied.

Furthermore, re-profiling of wheels and rails are performed to reduce dynamic variations of contact points, to guarantee stability during curving and to avoid derailment.

The basic model is used to investigate how the change in wheel-rail profile shape influences rail wear. Figures 5, 6 and 7 show the cross-sectional view of the wheel and rail profiles used in the simulations and Table 1 gives an overview of six combinations for wheel and rail profiles in various worn conditions. The worn rail profile (Figure 5) is measured at the critical value (vertical wear is equal to 12.5 mm) that triggers replacement of the track (hence the RUL is zero) and the mid rail profile is measured when the wear depth value is equal to approximately half the critical value. Two different wheel geometries are investigated i.e. s1002 and HIT. The worn wheel profile (Figure 6) of s1002 is adopted from (Dollevoet, 2010) which was measured after 1.5 years of operation. The worn HIT profile (Figure 7) was provided by Nedtrain and was measured just before re-profiling, which took place after three months of operation. The simulations of the wheel-

Table 1. Wheel-rail combinations.

	new wheel	worn wheel
new rail	×	×
mid rail	×	×
worn rail	×	×

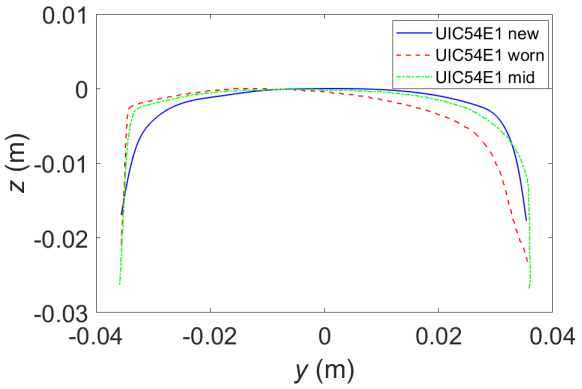

Figure 5. Rail profile UIC54E1 in new, mid and worn condition. (for the mid and worn profile, inclination (1/40) of the track is included in the shown profiles.)

rail combinations were furthermore performed on moderate curved tracks of radii varying from 1000 to 4000 meters and at a vehicle speed of 30m/s. The track curvature (i.e. the inverse of the radius) variation of a curve with radius R equal to 1000 meters is shown in Figure 8. The track layout in this simulation consists of a uniform rail profile where the first 50 meters of the track is straight with zero cant angle. Then after 50 meters the transition curve starts leading to the actual curve at a cant angle of 0.1 radians. The new rail profile is

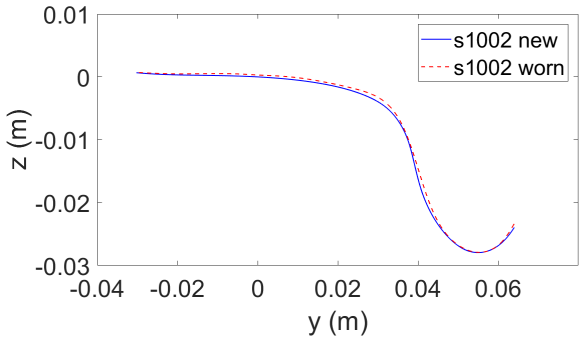

Figure 6. Wheel profile s1002 in new and worn condition.

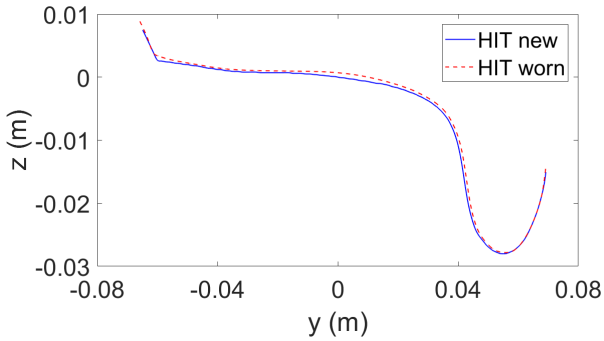

Figure 7. Wheel profile HIT in new and worn condition.

inclined at 1/40 and zero inclination is defined for the worn and mid rail profiles as the inclination was already included in the profile measurement. Configuration 1 in Figure 9 shows a cross section of a track layout without cant and configuration 2 with cant. Also the inclination is shown in the figure, where the angle of inclination is equal to 1/40 radians.

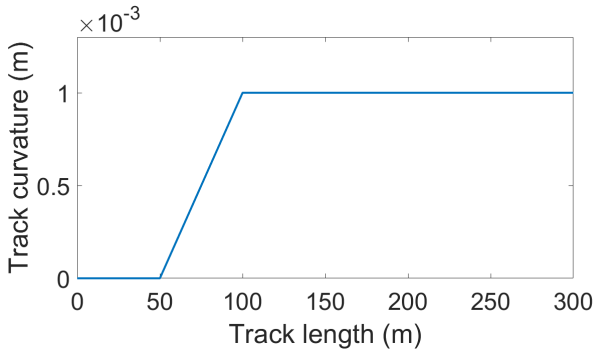

Figure 8. Track curvature.

2.4.2. Case study

The vehicle and track model used for the case study are similar to the ones shown in Figures 4 and 8. The case study takes into account the number of wheel passages and locally measured UIC54E1 rail profiles with 260Mn steel grade. In

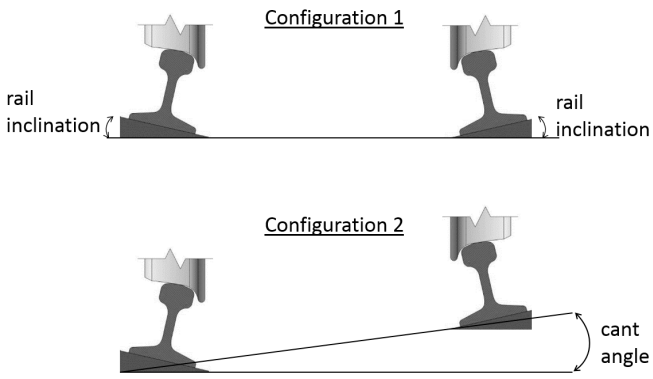

Figure 9. Schematic representation of rail inclination and cant angle (adapted from (Dollevoet, 2010)).

this case, the railway track between the cities of Weesp and Almere was chosen for studying a period of approximately three years (begin of 2014 – end of 2016). According to the train passages register provided by the Dutch Railways most of the trains that passed this route were the Sprinter Light Trains (SLT) and 'Verlengd InterRegio Materieel' (VIRM) trains with s1002 and HIT wheel profiles, respectively.

Three curves were selected for the case study: two right hand sided curves and one left hand sided curve with curve radius 1500 and 2500 meters, and 1800 meters, respectively. More information on the track layout can be found in Table 2. A minus sign in front of 1800 meters indicates that this curve is left hand sided. Furthermore, the track layout is composed of variable rail profiles measured at every 100 meters and the vehicle speed during the simulations is set to 38 m/s. The measured rail profiles were provided by Strukton Rail. The method for measuring these profiles will be discussed in the next subsection.

Table 2. Track layout characteristics for the case study.

Track layout	**1**	**2**	**3**
Curve radius(m)	1500	-1800	2500
Straight track length(m)	55	385	240
Transition curve length (m)	172	140	150
Actual curve length (m)	938	1200	1500
Cant angle (radians)	0.07	0.07	0.06

2.5. Rail Profile Measurement and Analysis Method

Rail profiles are measured and recorded by Eurailscout using the UFM 120 track recording car (Esveld, 2001). This type of train is fully equipped with laser scanning systems, cameras, GPS and other positioning methods which enables non-contact measurements of gauge variations, superelevation (cant) and rail profiles. The maximum vehicle speed is equal to 120 km/h and data sampling takes places every three meters. Hence every three meters rail profiles on both sides of the track are measured and recorded. Absolute wear area loss calculations (in mm^2) from raw data of the measurement train were unsuccessful due to the measurement error. This error is equal to ± 0.5 mm, while the vertical wear on the rail head can be in the same order or even less than 0.5 mm. Thus, determination of wear area loss is achieved by profile wear calculations derived from the European standard which has been published to support rail re-profile or rail grinding decisions (Vermeulen, Beltman, & Nauw, 2016). This method determines the amount of wear (in mm^2) that is worn off (in a 2D cross sectional view) with regard to the nominal/reference rail profile. It assesses the amount of material on the measured profile which deviates from the nominal profile after fitting the measured profile to the nominal profile over the points A (highest point of profile) and B ($\pm$ 14mm below point A), see Figure 10. Furthermore, the method assesses the worn area (in mm^2) for the inner (running/gauge) side and the outer (field) side of the rail separately. The reference line used to separate the inner and outer side of the rail is the line through the center of the nominal profile, and reference point A. The most right-hand side (RHS) section of the rail (for a RHS profile) is not included in the calculation. It is argued that there will be hardly any wheel-rail contact in this area, hence there will be no material loss. The 5 degree and 70 degree lines are used to bound the region for most likely to occur wheel-rail contact points. Figure 11 shows how the 5 and 70 degree lines are defined, these lines are perpendicular to the lines that make an angle of 5 and 70 degrees with the profile (Standard, 2009). The difference in area between the reference and measured profile at the gauge and field side is assumed to be equal to the worn area of gauge and field side, respectively. The final total wear of the rail head is then equal to the sum of the gauge and field side worn area. Although the results from this method can be argued to be unequal to the absolute worn area, for the purpose of validation of the simulated results they are used as the lower-bound.

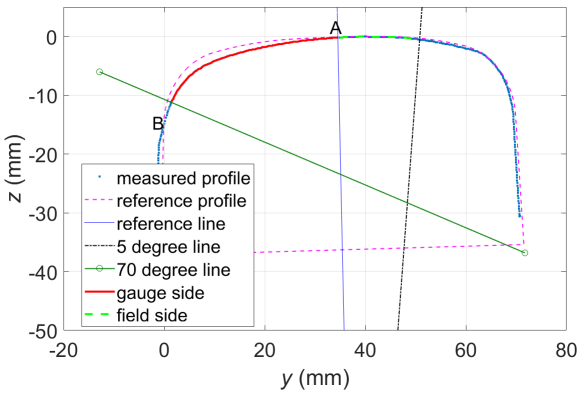

Figure 10. Cross sectional profile wear calculation method (Vermeulen et al., 2016).

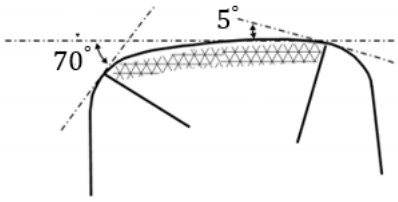

Figure 11. Definition of 5 and 70 degree lines. (Standard, 2009).

3. RESULTS AND DISCUSSION

In this section the results of the proposed method are presented and discussed. First, the basic model is used to obtain some generic insights and sensitivities. After that, the method is applied in a specific case study, and the results are validated with measurements on a real track section.

3.1. Basic Model

The wear area, caused by a single ERRI Wagon passage, versus the location on the track having a curve radius of 1000 meters is plotted in Figure 12. Only new s1002 wheel profiles have passed the RHS curved track consisting of new UIC54E1 rail profiles. The results show that the outer rail (w1l) experiences higher amount of material loss compared to the inner rail (w1r). These results can be explained by understanding the dynamic behavior of the wheelset. Due to the conicity of the wheels one side (side of the outer rail) will have a larger rolling radius than the other during curving. However, they have the same angular velocity and the wheelset is forced to yaw about the vertical axis. This introduces creep forces that try to get the vehicle back to the central position of the track (Wickens, 1965). As the creep forces are higher on the outer rail, that rail is wearing at a higher rate. Furthermore, results also show that the wear area depends on the location of the wheel in the bogie. The first wheel of the front bogie on the left-hand side (w1l front) generates more wear on the rail than the second wheel (w2l front). The same conclusion has been drawn for the rear bogie. This is again caused by differences in creepages caused by the wheels due to varying yaw angles and rolling radii of the wheels. As the track layout consisted of a straight, transition and actual curved part, the difference in generated wear area is as expected. The wear area generated on the actual curve (>100 m) is far more pronounced than on the straight part (0 – 50 m), since the rolling radius difference between left and right wheels are minimal for the straight track. The same results as shown in Figure 12 are also generated for curved tracks with radii varying from 1000 to 4000 meters. The average wear area calculated for only the actual curve part (see Figure 8) as function of curve radii is plotted in Figures 13 and 14. These plots show the results for different rail profiles in combination with varying s1002 and HIT wheel profiles, respectively. The results show that the new-new combinations generate the least amount of wear. This is as expected because wheel and rail profile geometries are optimized (during the design phase) such that the dynamic motion of the train is minimal. The highest amount of wear is generated for the worn rail - new wheel combinations. From these figures, it can also be seen that the wear for the curves with smaller radii is more pronounced than for the larger radii curves. The results give a good insight into the wear behavior but cannot give an accurate prediction of the wear rate yet, because the rail profiles used for the simulation are measured at random locations and left and right rails are assumed to be identical and uniform. To develop a method that is able to accurately predict the wear rate, a case study analysis is conducted for rail profiles measured at a specific location over a certain period.

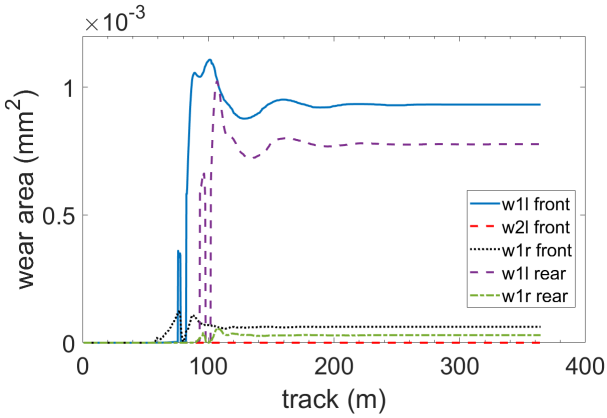

Figure 12. Wear area as function of the location on a curved track with radius R=1000m for the combination of UIC54 new and s1002 new. Curves for 5 different wheels of one wagon are presented: 3 wheels of the front bogie (first and second wheel on LHS (w1l front and w2l front, respectively) and first wheel on RHS (w1r front), and 2 wheels of the rear bogie (first wheel on LHS (w1l rear) and RHS (w1r rear)).

3.2. Case Study

The rail profiles on the Weesp – Almere railway line have been measured six times in the period of 2014 – 2016. Figures 15 until 17 show the results for measured and simulated wear area for the three chosen curves of the case study, namely the curves with radii R=1500m, R=-1800m and R=2500m. The measured wear is obtained by calculating the difference between the relative wear area of two consecutively performed measurements. The relative wear area is defined as the difference in wear area between measured and reference profile (in this case the new UIC54E1 profile) as was discussed in section 2.5. For example, relative wear area of the measurements performed in October 2014 are compared with relative wear area calculated from previous measurements performed in April 2014, to determine the change or increase in wear

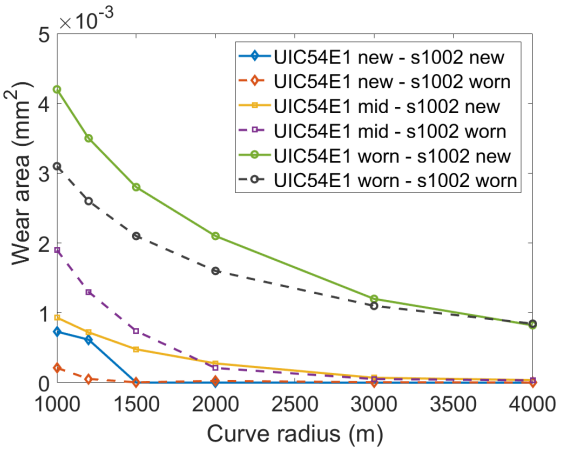

Figure 13. Maximum wear depth as function of curve radii for different s1002 wheel-rail combination.

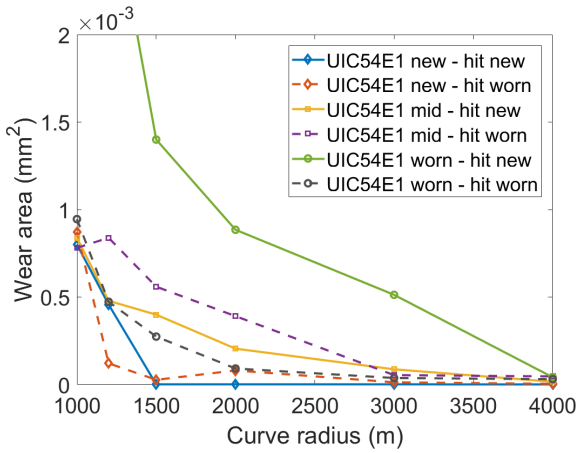

Figure 14. Maximum wear depth as function of curve radii for different HIT wheel-rail combination.

area between two measurements.

The UFM120 recording car yields a measured rail profile every three meters, hence there will be relative wear area values for every three meters on the track (for each measurement period). However, the measurement locations will not be identical for two different periods. Therefore, the comparison between two measurement periods are done such that the minimum distance in location of the two measured profiles is at most one meter. For example, a profile measured in April 2014 at kilometer 2.500 is compared with a profile measured in October 2014 at kilometer 2.501. The measured results shown in the Figures 15 until 17 represent the average wear area as obtained from the total number of rail profiles measured on the curve.

As mentioned in section 2.4.2, the track model for the case study consists of variable rail profiles such that every 100 meters the rail profile is changed. Then two type of simulations are carried out with this track model; in the first simulation only new wheel profiles run over the track, in the second one only worn wheels. The simulation results are then multiplied by the number of first wheel (w1) passages (of both, front and rear bogie) and corrected on the actual measured axle load. The number of wheel passages is extracted from the information received from the Dutch Railways. They provided the type of vehicles that passed on the track section of the case study with each type of vehicle containing the information of wheel profiles. Then the number of passed wheels for every type of wheel is established by only considering the number of front wheels of the bogie. This is because from the basic model it can be concluded that only the first wheel of the bogies are dominant for rail wear, see Figure 12.

The correction on axle load is performed in order to make the simulations representative for the specific case study, because the actual vehicles VIRM and SLT are not modelled in VI-Rail. The ERRI wagon is used as vehicle model and only its wheels are changed to either s1002 or HIT (in both new and worn condition) and the wagon mass is adjusted to either VIRM or SLT.

Some interesting findings from the basic model also apply to the case study. For example, from the Figures 15 until 17 it can be seen that curves with larger radii like R=2500m experiences less wear compared to R=1500m. Furthermore, it can be concluded that when only new wheels pass the track, the wear is much more pronounced than when worn wheels pass the track. The results of the latter simulation are also closer to the relative wear obtained from field measurements. The reason behind this is that the wear rate of wheels are higher compared to wear rates of rail (Nilsson, 2005; Dirks, 2015), because the wheel experiences more contact points due to its traveling over thousands of kilometers. Thus, most of the wheels that run over the tracks are already in worn condition.

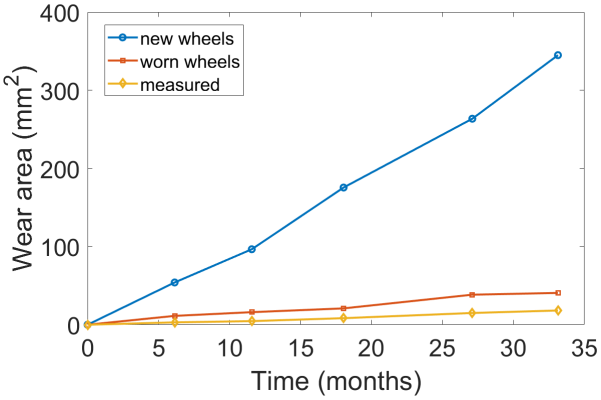

Figure 15. Outer rail wear area vs time for a curve with R=1500m.

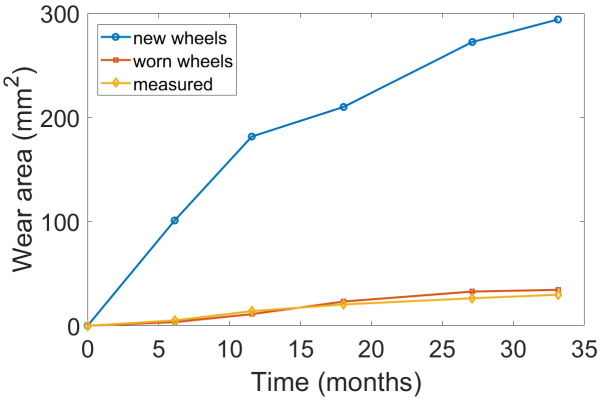

Figure 16. Outer rail wear area vs time for a curve with R=-1800m.

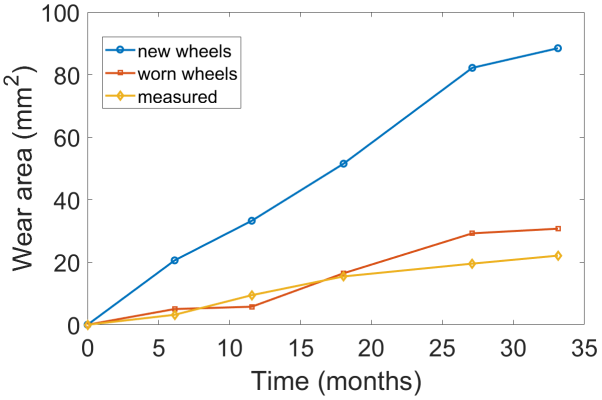

Figure 17. Outer rail wear area vs time for a curve with R=2500m.

4. CONCLUSION

This study proposes a strategic method that reduces the required computation time for rail wear prediction on moderate curves by omitting the rail profile update procedure and taking into account a specific set of operating conditions. The initial condition of the rail track in this case is defined by measured rail profiles rather than new rails. Results show that running worn wheels on the track in the simulation predicts a wear rate close to the measured wear, where the measured wear can be regarded as a lower-bound and simulations with new wheels as the upper-bound. Absolute wear area difference values are expected to be in-between these bounds. Hence, it can be concluded that the simulated results are reliable. However, one of the main challenges remains the detailed validation of the calculation method regarding the absolute wear area, which is complicated by the lack of detailed measurements of rail profiles.

The next step is to investigate the influence of the actual variations in usage like specific train type, vehicle speed, track geometry irregularities, etc.. For this purpose the research will be continued by performing a sensitivity analysis in order to find dominant operating parameters followed by developing meta-models which take into account the resulting parameters. In this way a decision support tool for infrastructure managers can be developed such that they do not have to perform simulations for each case.

ACKNOWLEDGMENT

This research has been conducted within the In2Rail project (European Union (EU) Horizon 2020 research and innovation program, grant agreement 635900) as lighthouse project to Shift2Rail research program, to be continued within the Shift2Rail project In2Smart (EU Horizon 2020 research and innovation program, grant agreement 730569). Furthermore, the authors would like to thank Strukton Rail for the financial support. The authors would also like to acknowledge David Vermeij from Stukton Rail and his team for the fruitful discussions on rail maintenance in practice and for providing real track data. Finally, the authors are very grateful for the help they received from Frank Vermeulen regarding wear calculations from measurements.

NOMENCLATURE

A	wear area [mm^2]
a	semi-axis a of contact area [mm]
b	semi-axis b of contact area [mm]
C_{11}, C_{22}, C_{33}	creepage coefficients [-]
F_N	normal contact force [N]
G	shear modulus [N/mm^2]
g	traction bound [N/mm^2]
H	material hardness [N/mm^2]
h	wear depth [mm]
K	wear coefficient [-]
L	single weighted parameter [m/N]
L_x, L_y, L_ϕ	flexibility parameters [m^3/N]
V	amount of wear volume [mm^3]
$V_{vehicle}$	vehicle speed [m/s]
p	contact pressure distribution [N/mm^2]
p_{max}	maximum contact pressure [N/mm^2]
q_t	tangential force [N]
q_x	x-component of tangential force [N]
q_y	y-component of tangential force [N]
R	curve radius [m]
s	sliding distance [mm]
V	vehicle speed [m/s]
v	sliding velocity [m/s]
γ_x	longitudinal creepage [-]
γ_y	lateral creepage [-]
ϕ	spin creepage [1/mm]
μ	friction coefficient [-]

REFERENCES

Archard, J. F. (1953). Contact and rubbing of flat surfaces. *Journal of Applied Physics*, *24*(8), 981-988. doi: 10.1063/1.1721448

De Arizon, J., Verlinden, O., & Dehombreux, P. (2007). Prediction of wheel wear in urban railway transport: comparison of existing models. *Vehicle System Dynamics*, *45*(9), 849-866. doi: 10.1080/00423110601149335

Dirks, B. (2015). *Simulation and measurement of wheel on rail fatigue and wear* (PhD Thesis).

Dollevoet, R. (2010). *Design of an anti head check profile based on stress relief* (PhD Thesis).

Enblom, R. (2005). *On simulation of uniform wear and profile evolution in the wheel - rail contact* (PhD Thesis).

Enblom, R., & Berg, M. (2008). Proposed procedure and trial simulation of rail profile evolution due to uniform wear. *Proceedings of the Institution of Mechanical Engineers Part F-Journal of Rail and Rapid Transit*, *222*(1), 15-25. doi: 10.1243/09544097jrrt173

Esveld, C. (2001). *Modern railway track* (second ed.). MRT-Productions.

Ignesti, M., Innocenti, A., Marini, L., Meli, E., & Rindi, A. (2014). A numerical procedure for the wheel profile optimisation on railway vehicles. *Journal of Engineering Tribology*.

Iwnicki, S. (2006). *Handbook of railway vehicle dynamics*. CRC Press.

Jendel, T. (2002). Prediction of wheel profile wear-comparisons with field measurements. *Wear*, *253*(1-2), 89-99. doi: 10.1016/S0043-1648(02)00087-X

Kalker, J. J. (1990). *Three-dimensional elastic bodies in rolling contact* (first ed.). Springer Netherlands.

Lewis, R., & Olofsson, U. (2004). Mapping rail wear regimes and transitions. *Wear*, *257*(7-8), 721-729.

Li, Z., & Kalker, J. J. (1998). Simulation of severe wheel-rail wear. *Computers in Railways*, *2*, 393-402.

Nilsson, R. (2005). *On wear in rolling/sliding contacts* (PhD Thesis).

Orvnas, A. (2005). *Simulation of rail wear on the swedish light rail line tvarbanan* (Master Thesis).

Pearce, T. G., & Sherratt, N. D. (1991). Prediction of wheel profile wear. *Wear*, *144*(1-2), 343-351. doi: 10.1016/0043-1648(91)90025-P

Santamaria, J., Herreros, J., Vadillo, E., & Correa, N. (2013). Design of an optimised wheel profile for rail vehicles operating on two track gauges. *Vehicle System Dynamics*, *51*, 54-73.

Shevtsov, I. (2008). *Wheel/rail interface optimisation* (Phd Thesis).

Sichani, M. S. (2016). *On efficient modelling of wheel-rail contact in vehicle dynamics simulation* (PhD Thesis).

Standard, E. (2009). *Railway applications - track - acceptance of works - part 3: Acceptance of reprofiling rails in track - pren13231-3* (Report).

Vermeulen, F., Beltman, B., & Nauw, R. (2016). *Description cross sectional profile* (Report). Eurailscout.

Vi-rail 17.0 documentation (Report). (2016).

Ward, A., Lewis, R., & Dwyer-Joyce, R. S. (2003). Incorporating a railway wheel wear model into multi-body simulations of wheelset dynamics. *Tribology Series*, *Volume 41*, 367-376.

Wickens, A. H. (1965). The dynamic stability of railway vehicle wheelsets and bogies having profiled wheels. , *1*, 319-341. doi: 10.1016/0020-7683(65)90037-5

Zobory, I. (1997). Prediction of wheel/rail profile wear. *Vehicle System Dynamics*, *28*(2-3), 221-259. doi: 10.1080/00423119708969355

BIOGRAPHIES

Annemieke Meghoe is a PhD student in the chair of Dynamics Based Maintenance at the University of Twente. She obtained her Bachelor of Science degree in Mechanical Engineering at the Anton de Kom University of Suriname and in 2015 she received her Master of Science degree in Mechanical Engineering at the University of Twente. She started with her PhD project 'Physical Model Based Predictive Maintenance for Rail-Infrastructure', in collaboration with Strukton Rail in September 2015.

Richard Loendersloot obtained his Master degree in Mechanical Engineering, research group Applied Mechanics, at the University of Twente in 2001. He continued as a PhD student for the Production Technology group of the University of Twente, researching the flow processes of resin through textile reinforcement during the thermoset composite production process Resin Transfer Moulding. He obtained his PhD degree in 2006, after which he worked in an engineering office on high end FE simulations of a variety mechanical problems. In 2008 he returned to the University of Twente as part time assistant professor for Applied Mechanics. From September 2009 on he holds a fulltime position. Since then, his research started to focus on vibration based structural health and condition monitoring, being addressed in both research and education. He became part of the research chair Dynamics Based Maintenance upon its initiation in 2012. His research covers a broad range of applications: from rail infra structure monitoring, to water mains condition inspection and aerospace health monitoring applications, using both structural dynamics and ultrasound methods. He is involved in a number of European and National funded research projects.

Rob Bosman studied mechanical engineering and tribology at the University of Twente in The Netherlands (MSc. 2007, Ph.D. 2011). He then worked at Pentair FairBanks-Nijhuis for 2 years as an R&D and reliability engineer, after which he returned to the university as an assistant professor and is currently an associate professor. Along with his professorship Bosman since 2014 has worked part-time at Shell Rijswijk

R&D as a research coordinator.

Tiedo Tinga received a Master degree in Applied Physics (1995) and a PDEng degree in Materials Technology (1998) at the University of Groningen. He did his PhD research during his work with the National Aerospace Laboratory NLR on the development of a multi-scale gas turbine material model. He received his PhD degree in 2009 from Eindhoven University of Technology. Since 2007 he has a position at the Netherlands Defence Academy, presently as a (part-time) full professor Life Cycle Management. Since 2012 he is also a full professor in Dynamics based Maintenance at the University of Twente. In both institutes he leads a research program on predictive maintenance, health and condition monitoring and life cycle management.

APPENDIX

Table 3. Vehicle characteristics of the ERRI Wagon.

Car body mass (kg)	32000
Distance between bogie pivots (m)	19
Primary suspension mass	
Bogie (kg)	2615
Wheelset (kg)	1503
Wheel radius (new) (m)	0.46
Wheel radius (fully worn) (m)	0.42
Primary vertical dampers	
Non-linear damping (N/m/s)	1000
Series stiffness (N/m)	6.0E+005
Primary suspension	
Longitudinal stiffness (N/m)	6.17E+005
Lateral stiffness (N/m)	6.17E+005
Vertical stiffness (N/m)	7.32E+005